



Numerical simulation of heat transfer in packed pebble beds: CFD-DEM coupled with particle thermal radiation

Hao Wu ^{a,b}, Nan Gui ^a, Xingtuan Yang ^a, Jiyuan Tu ^{a,b}, Shengyao Jiang ^{a,*}

^a Institute of Nuclear and New Energy Technology, Collaborative Innovation Center of Advanced Nuclear Energy Technology, Key Laboratory of Advanced Reactor Engineering and Safety, Ministry of Education, Tsinghua University, Beijing 100084, China

^b School of Engineering, RMIT University, Melbourne, VIC 3083, Australia



ARTICLE INFO

Article history:

Received 9 October 2016

Accepted 12 March 2017

Available online 23 March 2017

Keywords:

Particle

Gas particle flow

Thermal radiation

Packed pebble beds

CFD-DEM

ABSTRACT

Particle thermal radiation plays a significant role in many heat transport devices, such as pebble-bed high temperature gas-cooled nuclear reactors (HTGR). The effect of particle thermal radiation in packed pebble beds has been rarely investigated at particle scale. In this work, a complete CFD-DEM method coupled with particle-scale radiation is discussed for packed pebble beds, considering particle motion, fluid flow, particle-fluid interactions and heat convection, conduction and particle radiation. It is shown that, compared to the case without particle radiation, heat transfer is enhanced greatly by particle radiation at high temperatures. A particle radiation factor (PRF) is proposed as an independent non-dimensional parameter to qualify the effect of particle-scale radiation in packed pebble beds. The PRF increases significantly with temperature and decreases gradually as the heat storage capacity or the thermal conductivity of the fluid increases. A demonstrative utilization of the present model is performed for a benchmark problem based on the HTR-10 nuclear reactor, and the results in general are in agreement with the results predicted by other empirical codes. When the nuclear reactor is above full power, the power required by the fan will increase significantly. In the decay heat removal process, particle radiation is essential to keep the bed temperature below the allowable limit, which is significant for nuclear reactor safety.

© 2017 Elsevier Ltd. All rights reserved.

1. Introduction

A high temperature gas-cooled reactor (HTGR) is an advanced type of generation IV nuclear reactor. Due to their inherent safety and potential for hydrogen production [34], HTGRs are being deployed very quickly and intended to be commercialized for large-scale applications in the near future. The core of a HTGR is a packed pebble bed of random and dense packing consisting of mono-sized spherical pebbles and cooled by helium gas under high pressure, e.g. about 7 MPa for the HTR-PM nuclear reactor [31,6].

From the point of design and engineering applications, it is essential and very meaningful to simulate the flow and heat transfer processes in packed pebble beds. Before, a thorough understanding of the physical mechanisms involved in a packed bed was developed, and a pseudo-porous medium model was established to provide an empirical approach to analyze the steady state behavior during normal conditions and the transient behaviors during nuclear accidents of HTGRs [36]. Theoretically, the flow

through a packed pebble beds is complex gas-solid flow coupled with particle motion, fluid flow and the interactions between the particles. The CFD-DEM method is now fully developed and widely applied in granular flows and fluidized beds [20,35,10,11]. It combines computational fluid dynamics for the continuous phase and the discrete element method for the particle phase [38,42] and makes it possible to investigate the complex processes in a Eulerian-Lagrangian framework [37]. Moreover, it is also feasible to study the effect of non-spherical particles with different sizes and shapes for fluidized beds [12,39].

However, the heat transfer model for packed pebble beds needs to be improved substantially. Three basic modes of heat transfer need to be considered in simulations, i.e. conduction between particles in contact, fluid-particle convection and particle thermal radiation. In many cases, only the conduction and convection models are applied and particle radiation is neglected for low temperature conditions [15,24]. However, when the operating temperature of a packed pebble bed is very high (about 1100 K) at normal conditions and the particle size is large (60 mm in diameter), particle thermal radiation plays a significant role in the heat transport processes [13,30]. From all available literature on the CFD-DEM method, only a simplified radiation model [33,40] is

* Corresponding author.

E-mail addresses: guinan@mail.tsinghua.edu.cn (N. Gui), shengyaojiang@sina.com (S. Jiang).

Nomenclature

A	area (m^2)	$\delta\mathbf{n}, \delta\mathbf{t}$	deformations in the normal and tangential directions
a, b, B, C	temporary constants	θ	non-dimensional temperature difference
C_d	drag coefficient	ϑ	standard deviation of temperature (K)
C_p	fluid specific heat ($\text{J kg}^{-1} \text{K}^{-1}$)	λ	conductivity ($\text{W m}^{-1} \text{K}^{-1}$)
C_{pp}	particle specific heat ($\text{J kg}^{-1} \text{K}^{-1}$)	Λ	non-dimensional solid conductivity
d	particle diameter (m)	μ_f	viscosity (Pa s)
e	coefficient of restitution	μ_p, μ_r	friction and rolling friction coefficients
E	Young's modulus (Pa)	ν	Poisson ratio
F	force (N)	ρ	density (kg/m^3)
g	gravity (m/s^2)	σ	Stefan–Boltzmann constant ($5.670367 \times 10^{-8} \text{ W m}^{-2} \text{ K}^{-4}$)
G	shear modulus (Pa)	τ	non-dimensional temperature drop
h	heat convection coefficient ($\text{W m}^{-2} \text{ K}$)	φ	particle radiation factor
H	heat transfer coefficient (W/K)	ε	surface emissivity
I	moment of inertia (kg m^2)	ω	angular velocity (rad/s)
k	elastic constants (N/m)		
k_{eff}	effective thermal conductivity		
L	distance between two particles (m)		
m	mass (kg)		
M_r	rolling friction torque (N m)		
Nu	Nusselt number		
p	pressure (Pa)		
Pr	Prandtl number		
q	heat flux (W)		
Q_m	mass flow rate (kg/s)		
R	particle radius (m)		
Re	Reynolds number		
S_m	momentum source term (Pa/m)		
S_e	energy source term (W/m^3)		
t	time (s)		
T	temperature (K)		
u	fluid velocity (m/s)		
V	particle velocity (m/s)		
\tilde{V}	view factor		
V_{cell}	cell or control volume (m^3)		
x	radial distance to the center line (m)		
<i>Greek letters</i>			
α	porosity	c	conduction
β	damping coefficient	e	energy
γ	viscoelastic damping constant	f	fluid
γ_{pf}	coefficient of particle-fluid interaction ($\text{Pa m}^{-2} \text{ s}$)	i, j, k	particle index
		m	momentum
		n	normal direction
		p	particle
		r	radiation or rolling
		s	source term or sphere
		t	tangential direction
<i>Abbreviations</i>			
CFD	computational fluid dynamics		
DEM	discrete element method		
HTGR	high temperature gas-cooled reactor		
HTR-10	high temperature reactor with 10 MWt		
HTR-PM	high temperature gas-cooled reactor pebble-bed module		
INET	Institute of nuclear and new energy technology		
LRM	long-range radiation model		
PRF	particle radiation factor		
SRM	short-range radiation model		

available, where the averaged surrounding temperature [16] is replaced by a local environmental temperature. By comparison with other modes of heat transfer, particle radiation will increase significantly at high temperatures [40]. However, the effect of material thermal conductivity on particle radiation is not considered in this model. Moreover, the radiation model has not been verified separately for packed pebble beds. Thus, a new radiation model with an acceptable level of accuracy in engineering is needed for packed pebble beds.

In our previous work [30], particle thermal radiation was analyzed in detail (with radiation only and without thermal conduction) for packed pebble beds and three numerical models of different spatial scales were proposed. In the long-range radiation model (LRM), all possible heat transfer by radiation between surrounding particles is taken into account. However, from numerical results, the predicted heat flux from the long-range radiation model is much higher than experimental data because of the ignorance of the material conductivity which could be viewed as an inner thermal resistance for radiation. In the short-range radiation model (SRM), only thermal radiation between direct Voronoi neighbors are considered and it is in better agreement with exper-

imental data than the LRM. Because, in the SRM, the under prediction of radiation caused by the ignorance of long-range radiation heat exchange cancels out the over prediction of heat flux caused by the ignorance of inner thermal resistance, which results in better predictions of the overall radiation in packed pebble beds.

Therefore, based on the short-range radiation model, a complete CFD-DEM method was developed for packed pebble beds in the present work. Simulations with different initial conditions or physical properties were performed. The effect of particle thermal radiation in packed pebble beds is discussed using dimensional analysis. Then, the present SRM-based CFD-DEM model is assessed and resulted to be suitable for engineering applications, especially for HTGRs.

2. Numerical model

2.1. Governing equations

For the incompressible fluid phase, the mass, momentum and energy conservation equations are given as follow [28,35,40]

$$\frac{\partial(\rho_f \alpha_f)}{\partial t} + \nabla \cdot (\rho_f \alpha_f \mathbf{u}_f) = 0 \quad (1)$$

$$\frac{\partial(\rho_f \alpha_f \mathbf{u}_f)}{\partial t} + \nabla \cdot (\rho_f \alpha_f \mathbf{u}_f \mathbf{u}_f) = -\alpha_f \nabla p + \nabla \cdot (\mu_f \alpha_f \nabla \mathbf{u}_f) + \mathbf{S}_m \quad (2)$$

$$\frac{\partial(\rho_f C_p \alpha_f T_f)}{\partial t} + \nabla \cdot (\rho_f C_p \alpha_f \mathbf{u}_f T_f) = \nabla \cdot (\lambda_f \alpha_f \nabla T_f) + S_e \quad (3)$$

where ρ_f and α_f are the fluid density and porosity. \mathbf{u}_f and T_f are the fluid velocity and temperature. p and μ_f are the pressure and fluid viscosity. C_p and λ_f are the specific heat and thermal conductivity. \mathbf{S}_m and S_e are the momentum and energy source terms respectively. For particle motion, the discrete element method (DEM) now is accepted as an effective approach for simulation, which was originally developed by Cundall and Strack [5]. The translational and rotational equations for particle i at time t are given as [20,38,40]

$$m_i \frac{d\mathbf{V}_i}{dt} = m_i \mathbf{g} + \sum_{j=1}^n (\mathbf{F}_{n,ij} + \mathbf{F}_{t,ij}) + \mathbf{F}_{f,i} \quad (4)$$

$$I_i \frac{d\boldsymbol{\omega}_i}{dt} = \sum_{j=1}^n (\mathbf{R}_i \times \mathbf{F}_{t,ij}) + \sum_{j=1}^n \mathbf{M}_{r,ij} \quad (5)$$

where m_i, I_i are the mass and moment of inertia of particle i . \mathbf{V}_i and $\boldsymbol{\omega}_i$ are the translational and angular velocity vectors respectively. $m_i \mathbf{g}$ is the gravitational force. $\mathbf{F}_{n,ij}$ and $\mathbf{F}_{t,ij}$ are the normal and tangential contact forces to particle j . $\mathbf{F}_{f,i}$ is the particle-fluid interaction force. $\mathbf{M}_{r,ij}$ is the rolling friction torque to particle j . In the Hertz-Mindlin contact model [14] with directional constant torque [2], the forces and torque for the sticking contact surfaces are expressed as

$$\mathbf{F}_{n,ij} = k_n \delta \mathbf{n}_{ij} - \gamma_n \mathbf{V}_{n,ij} \quad (6)$$

$$\mathbf{F}_{t,ij} = k_t \delta \mathbf{t}_{ij} - \gamma_t \mathbf{V}_{t,ij} \quad (7)$$

$$\mathbf{M}_{r,ij} = -\frac{\omega_{ij}}{|\omega_{ij}|} \mu_r R_i F_{n,ij} \quad (8)$$

where $\mathbf{V}_{n,ij}$ and $\mathbf{V}_{t,ij}$, k_n and k_t , γ_n and γ_t , $\delta \mathbf{n}_{ij}$ and $\delta \mathbf{t}_{ij}$ are the relative velocity, elastic constants, viscoelastic damping constants and deformations in the normal and tangential directions, respectively. μ_r is the coefficient of rolling friction. When $\mathbf{F}_{t,ij} > \mu_p \mathbf{F}_{n,ij}$, the contact surfaces are sliding and $\mathbf{F}_{t,ij} = \mu_p \mathbf{F}_{n,ij}$, where μ_p is the friction coefficient. The elastic and viscoelastic damping constants are formulated as

$$k_n = \frac{4}{3} E^* \sqrt{R^* \delta \mathbf{n}_{ij}} \quad (9)$$

$$k_t = 8G^* \sqrt{R^* \delta \mathbf{n}_{ij}} \quad (10)$$

$$\gamma_n = -2 \sqrt{\frac{5}{6}} \beta \sqrt{\frac{3}{2}} k_n m^* \quad (11)$$

$$\gamma_t = -2 \sqrt{\frac{5}{6}} \beta \sqrt{k_t m^*} \quad (12)$$

where β is the damping coefficient. E^* , G^* , R^* and m^* are equivalent values of the Young's modulus [41], shear modulus, radius and mass, which are given by

$$\frac{1}{m^*} = \frac{1}{m_i} + \frac{1}{m_j} \quad (13)$$

$$\frac{1}{R^*} = \frac{1}{R_i} + \frac{1}{R_j} \quad (14)$$

$$\frac{1}{E^*} = \frac{1 - v_i^2}{E_i} + \frac{1 - v_j^2}{E_j} \quad (15)$$

$$\frac{1}{G^*} = \frac{2(2 - v_i)(1 + v_i)}{E_i} + \frac{2(2 - v_j)(1 + v_j)}{E_j} \quad (16)$$

where v is the Poisson ratio of the particle material. The damping coefficient can be obtained from

$$\beta = \frac{\ln(e)}{\sqrt{\pi^2 + \ln^2(e)}} \quad (17)$$

where e is the coefficient of restitution.

2.2. Heat transfer modeling

The equation for the conservation of energy for particle i can be expressed as

$$m_i C_{pp,i} \frac{dT_{p,i}}{dt} = \sum_{j=1}^n q_{c,ij} + \sum_{k=1}^m q_{r,ik} + q_{f,i} + q_{s,i} \quad (18)$$

where $m_i, C_{pp,i}$ and $T_{p,i}$ are the particle mass, specific heat and temperature. $q_{c,ij}$ is the heat conduction flux to particle j and n is the number of particles in contact with particle i . $q_{r,ik}$ is the thermal radiation flux to particle k and m is the number of particles connected to particle i by thermal radiation. $q_{f,i}$ and $q_{s,i}$ are the heat flux by fluid convection and the heat source term.

For particle heat conduction, the heat flux between two particles in contact is calculated as [9,35,40]

$$q_{c,ij} = H_{ij}(T_j - T_i) \quad (19)$$

where H_{ij} is heat transfer coefficient which is determined by the physical properties of the particles, surface roughness and relative position to particle j [27,8]. H_{ij} can be obtained from experimental measurements or the equation which is written as [15]

$$H_{ij} = \frac{4}{1/\lambda_i + 1/\lambda_j} \sqrt{A_{c,ij}} \quad (20)$$

where λ_i and λ_j are thermal conductivities of particles i and j . $A_{c,ij}$ is the contact area between the pair.

By contrast, the particle thermal radiation in a packed pebble bed of dense packing consists of non-contact and long-range interactions. It was proven by theoretical calculation [23] and experimental results [25] that the solid conductivity (λ_s) of particle material plays an important role in particle thermal radiation exchange of the packed pebble beds. The non-dimensional solid conductivity is defined as

$$\Lambda = \frac{\lambda_s}{4\sigma d_p T_s^3} \quad (21)$$

where σ is Stefan-Boltzmann constant. d_p and T_s are the diameter and temperature of the particle, respectively. The effect of solid conductivity on the particle radiation is negligible only at $\Lambda > 10$. The non-dimensional solid conductivity obtained from experimental measurements [22] is shown in Fig. 1. The effect of material conductivity on the particle radiation can be divided into three regions: (1). A low temperature region (Region I). In this region, the temperature is less than 550 °C and the heat flux of particle radiation is also very low. The long-range radiation considering all possible thermal radiation is valid strictly, in which every particle is assumed to be an isothermal body [30]. (2). A high temperature region (Region II). The temperature in this region is about 550–1262 °C in the

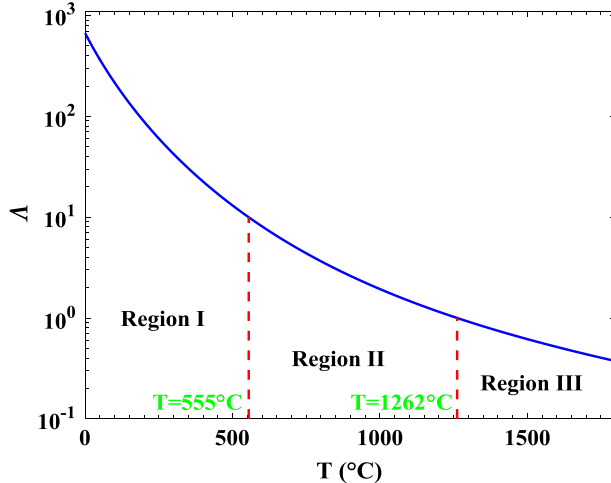


Fig. 1. Non-dimensional solid conductivity of the packed pebble beds under different operation temperatures for HTGRs.

core of HTGRs. The inner thermal resistance for particle radiation caused by solid conductivity increases greatly with temperature. In this region, the prediction obtained by the long-range radiation model will overestimate the radiation flux if the inner thermal resistance is omitted. (3). A super-high temperature region (Region III). The inner thermal resistance reaches almost a constant when temperature exceeds 1262 °C.

In most engineering applications, the highest temperatures of HTGRs are within region II. Thus the short-range radiation model is recommended for high temperature region. Moreover, as the pebble packing is very dense, particle radiation is blocked greatly by immediate neighbors. The radiation flux between two spheres that are far away from each other is very low. Therefore, in current short-range radiation model, only the neighboring Voronoi pairs very close to each other (Fig. 2) are considered for particle radiation. The Voronoi cell is used here to facilitate and simplify the calculation of view factors, since analytical calculation of the view factors for all possible packing structures is much more complicated than through the Voronoi cell. The heat flux between two neighboring particles is formulated as

$$q_{r,ik} = \frac{\sigma(T_k^4 - T_i^4)}{\frac{1-\varepsilon_i}{\varepsilon_i A_i} + \frac{1}{A_i \bar{V}_{i,k}} + \frac{1-\varepsilon_k}{\varepsilon_k A_k}} \quad (22)$$

where $\varepsilon_i, \varepsilon_k$ and A_i, A_k are surface emissivity and area of particle i and particle k . $\bar{V}_{i,k}$ is the modified view factor by considering the non-closed cavity and the effect of solid conductivity [30].

In engineering applications, the effective thermal conductivity for heat conduction between particles in contact (k_c) can be obtained from experimental data [22,32] or empirical correlations [3,25]. In an analogous approach, the Voronoi cell shown in Fig. 2b can be regarded as a porous cell similar to that in the continuum framework with the same mass of the particle. Then, the heat conduction between two Voronoi neighbors in current work can be simplified as

$$H_{ij} = k_c A_0 / L_0 \quad (23)$$

where L_0 is defined as the distance between the particle centers enclosed by neighboring cells and A_0 is the cross-sectional area of the connected cells (see Fig. 2b). Although H_{ij} can be obtained from Eq. (20), we prefer to use Eq. (23) since the effective thermal conductivity of particle-particle conduction (k_c) can be obtained from the experimental data [26].

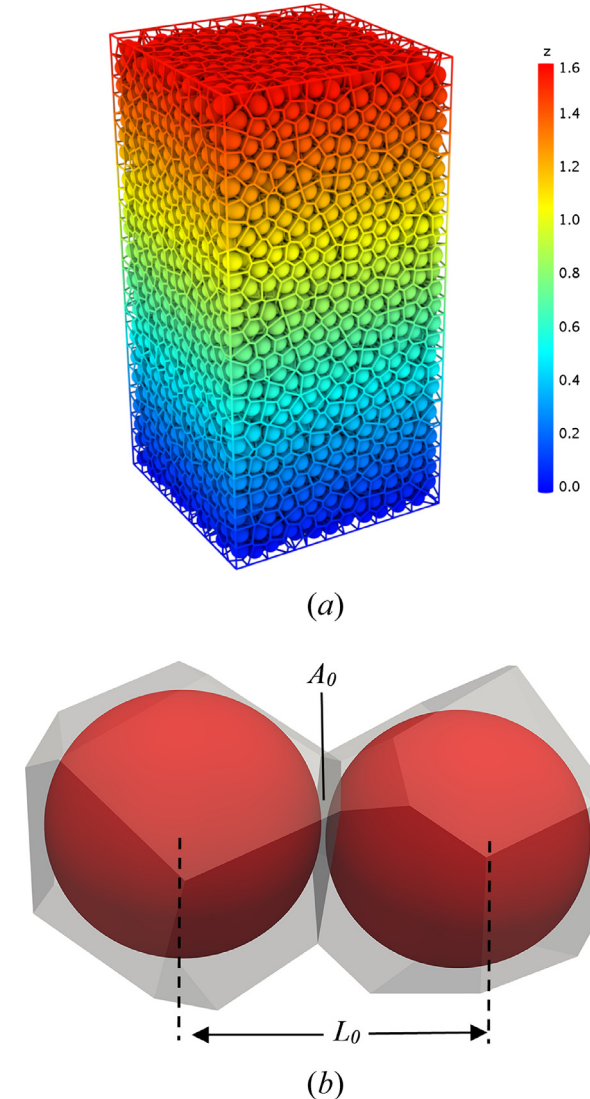


Fig. 2. Voronoi tessellation of a typical packed pebble bed (a) and a neighboring pair in the Voronoi cell(b) (the geometry is 0.8 m × 0.8 m × 1.6 m and z is z-coordination of particle position).

The particle radiation can be expressed and computed in a similar approach to the particle conduction. In a semi-empirical radiation model, the heat flux of particle radiation between two Voronoi cells is

$$q_{r,ik} = k_r A_0 (T_k - T_i) / L_0 \quad (24)$$

where k_r is effective thermal conductivity for particle radiation. There are a lot of efforts to obtain the correlations of k_r [25]. The reliable correlation for HTGR is the ZBS model [22], which is given by

$$k_r = 4\sigma d_p T^3 \left\{ [1 - \sqrt{1 - \alpha_f}] \alpha_f + \frac{\sqrt{1 - \alpha_f}}{2/\varepsilon - 1} \cdot \frac{B + 1}{B} \cdot \frac{1}{1 + 1/[(2/\varepsilon - 1)\Lambda]} \right\} \quad (25)$$

where $B = 1.25[(1 - \alpha_f)/\alpha_f]^{10/9}$. The ZBS model can be extended to very high temperature. Therefore, the semi-empirical radiation model (SEM) is applicable in the packed pebble beds for all temperature ranges (0–1600 °C) and is also adopted in the current work to be compared to the simulation result obtained from the short-range model (SRM).

The porosity, momentum source term and the particle-fluid interaction force in a CFD cell can be written as

$$\alpha_f = 1 - \frac{V_p}{V_{cell}} \quad (26)$$

$$\mathbf{S}_m = -\sum_{i=1}^n \mathbf{F}_{f,i}/V_{cell} \quad (27)$$

$$\mathbf{F}_{f,i} = -\gamma_{pf}(\mathbf{u}_f - \mathbf{V}_p) \quad (28)$$

where V_{cell} is the volume of the cell, and \mathbf{V}_p is the particle velocity. n is the number of particles inside the cell. γ_{pf} is a fluid-particle interaction coefficient [35,37,40]. Under normal conditions, the Gidaspow model [15] is suggested. For dilute particle flow ($\alpha_f > 0.8$), it is given as

$$\gamma_{pf} = \frac{3}{4} \rho_f C_d \frac{\alpha_f(1-\alpha_f)|\mathbf{V}_p - \mathbf{u}_f|}{d_p} \alpha_f^{-2.65} \quad (29)$$

$$C_d = \frac{24}{\alpha_f Re_p} [1 + 0.15(\alpha_f Re_p)^{0.687}] \quad (30)$$

where d_p is particle diameter. Re_p is particle Reynolds number that is defined as

$$Re_p = \frac{\rho_f |\mathbf{u}_f - \mathbf{V}_p| d_p}{\mu_f} \quad (31)$$

When $\alpha_f \leq 0.8$, the correlation is given as

$$\gamma_{pf} = 150 \frac{(1-\alpha_f)^2 \mu_f}{\alpha_f d_p^2} + 1.75 \rho_f \frac{(1-\alpha_f)|\mathbf{u}_f - \mathbf{V}_p|}{d_p} \quad (32)$$

For fluid-particle convection in a cell, the heat flux is expressed as

$$q_{f,i} = h A_p (T_f - T_i) \quad (33)$$

$$S_e = -\sum_{i=1}^n q_{f,i}/V_{cell} \quad (34)$$

where A_p is surface area of the particle and h is heat convection coefficient. It is important to predict h in numerical simulations, which basically given as

$$h = Nu \lambda_f / d_p \quad (35)$$

$$Nu = 2 + CR e_p^a Pr^b \quad (36)$$

where Nu and Pr are the Nusselt number and Prandtl number, respectively. C, a and b are constants for the particular geometrical structure [1,19]. Additional correlations are listed in Table 1.

3. Results and discussion

3.1. Model validation

In the present work, the experiment of Wen [29] is selected to validate the numerical model. The packed bed is a long cylindrical column with 1100 mm in length and 41 mm in internal diameter. It is filled with spherical glass particles with 5 mm in diameter and the average porosity of 0.4175. There was no heat source inside the particles and the wall temperature was maintained at 100 °C. Air at 20 °C was injected into packed bed from the bottom and thermocouples were used to measure the temperature field. The case with an inlet Reynolds number $Re = 328$ was simulated using a structured mesh (Fig. 3a).

The particles in the packed bed were heated by the hot wall and also cooled by the air flow. At steady state, the temperatures for both air and particles will increase along the flow direction. It is shown in Fig. 3b that air temperature distribution along the center line is in good agreement with the experimental data. Thus, it is concluded that the present model is valid for the simulation of flow and heat transfer of packed bed.

3.2. Simulation set-up for packed pebble bed

In the numerical simulations of the packed pebble bed, the geometry is a rectangular box (0.8 m × 0.8 m × 1.6 m). The granular system consisted of graphite spheres of 60 mm in diameter and the average porosity of 0.39, which is in accordance with the typical conditions found in a HTGR [34]. Initially, all particles were at the same high temperature and were cooled by fluid convection. The temperature of particles gradually decreased as no heat source was considered in the simulations. The packed bed and the CFD mesh are shown in Fig. 4 and the parameters employed in simulations are listed in Table 2, where the property parameters are assumed to be constants.

3.3. Dimensional analysis

Dimensional analysis is used to be able to compare the numerical results of the simulations with different initial and inlet temperatures. For every particle in the packed pebble bed, the non-dimensional temperature T^* is defined as

$$T^* = \frac{T_p - T_{in}}{T_{p,0} - T_{in}} \quad (37)$$

where $T_{p,0}$ and T_{in} are the initial particle temperature and flow inlet temperature respectively. The non-dimensional temperature drop τ of the packed pebble bed can be written as

$$\tau = 1 - \bar{T}^* \quad (38)$$

where \bar{T}^* is the arithmetic average of non-dimensional temperatures of all particles in the packed pebble bed. In the simulation, all the particles have the same properties. The Nusselt number is assumed to be constant too, since the fluid properties are assumed to be constant and there is no acceleration of the flow after the initial development of the fluid field at the inlet. Thus, the flow-particle heat convection coefficients for all particles are the same. At the start, all particles have the same temperature and $\tau = 0$. When all the particles have been cooled to fluid inlet temperature, τ will be 1. The numerical results for different initial temperatures with the same non-dimensional temperature drop ($\tau = 0.5$) are shown in Fig. 5. It can be seen that there is no notable difference between the non-dimensional particle temperature fields at low temperatures (less than 900 K), for which particle radiation flux is not dominant. However, the particle temperature fields tend to be much more uniform at high temperatures, since the heat transfer processes in packed pebble beds are enhanced by thermal radiation at high temperatures.

In order to quantify the effect of particle radiation in the heat transfer processes of packed pebble beds, the range of non-dimensional temperature for all particles is defined as

$$\theta = T_{max}^* - T_{min}^* \quad (39)$$

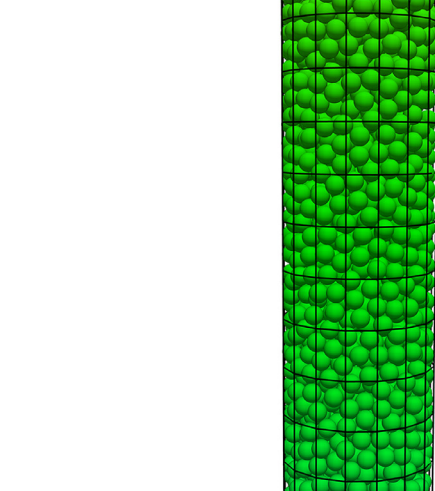
where T_{max}^* and T_{min}^* are the maximum and minimum of non-dimensional particle temperatures. The standard deviation also represents the quantity of data dispersion in statistics, which can be calculated as

Table 1

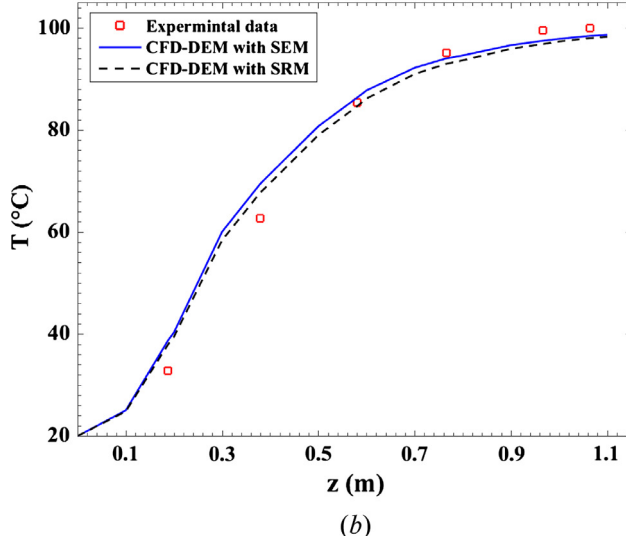
Correlations for particle-fluid interaction coefficient.

Authors	Expressions	Comments	Refs.
Wakao et al.	$Nu = 2 + 1.1Re_p^{0.6}Pr^{1/3}$	–	[1]
Ranz et al.	$Nu = 2 + 0.6Re_p^{0.5}Pr^{1/3}$	–	[19,35]
Kemp et al.	$Nu = 2 + 0.6Re_p^{0.5}Pr^{1/3} + 0.02Re_p^{0.8}Pr^{1/3}$	$200 < Re < 1500$	[19]
Bandrowski et al.	$Nu = 0.00114Re_p^{0.8159}\alpha_f^{0.5984}$	$180 < Re < 1800$ $2.5 \times 10^{-4} < \alpha_f < 0.05$	[19]
Zhou et al.	$Nu = 2 + 1.2Re_p^{0.5}Pr^{1/3}$	–	[40]
KTA standards	$Nu = 1.27Re_p^{0.36}Pr^{1/3}\alpha_f^{-1.18} + 0.033Re_p^{0.86}Pr^{1/2}\alpha_f^{-1.07}$	$10^2 < Re < 10^5$	[17]

3.2. Numerical simulation of the packed pebble bed

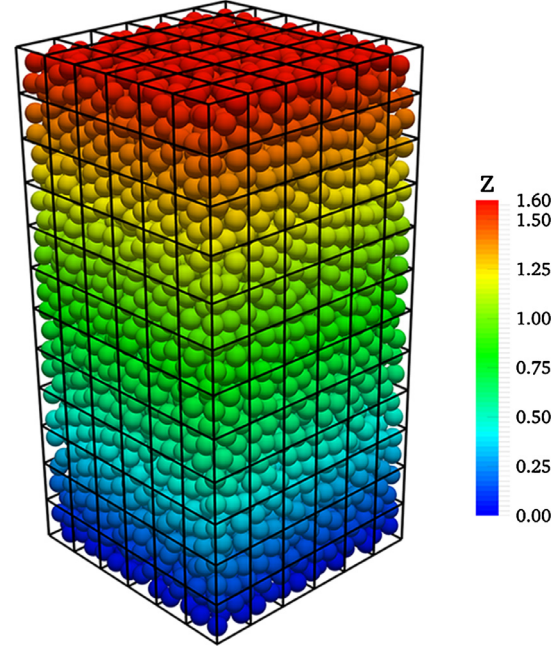


(a)

**Fig. 3.** Local view of particle packing and CFD mesh (a) and simulation result (b) for Wen's experiment at $Re = 328$. (Herein, the semi-empirical radiation model (SEM) applicable for all temperature ranges (0–1600 °C) is used to compare with the short-range model (SRM)).

$$\vartheta = \sqrt{\frac{1}{n} \sum_{i=1}^n (T_i^* - \bar{T}^*)^2} \quad (40)$$

From simulation results shown in Fig. 6, the values for the range ϑ as a function of the temperature drop τ increase from 0 at the start ($\tau = 0$) to its maximum at approximately $\tau = 0.5$ (the details of ϑ_{\max} and $\tau = \tau(\vartheta_{\max})$ are shown in Table 3). Then the values decrease

**Fig. 4.** Particle packing and CFD mesh in simulations for the packed pebble bed.**Table 2**
Parameters for simulation of the packed pebble bed.

Parameters (unit)	Value
Fluid (air) inlet velocity at bottom, u_{in} (m/s)	1.0
Fluid density, ρ_f (kg/m ³)	1.225
Viscosity, μ_f (Pa s)	1.79×10^{-5}
Fluid specific heat, C_p (J/(kg K))	1007
Fluid conductivity, λ_f (W/(m K))	0.0242
Flow directions	Upward or downward (for HTR-10)
Particle surface emissivity, ε	0.8
Effective conductivity of particle conduction, k_c (W/(m K))	4.0
Poisson ratio of particle material	0.45
Coefficient of restitution	0.3
Friction coefficient	0.5
Young's modulus (MPa)	50.0
Particle initial temperature, $T_{p,0}$ (K)	400, 600, 900, 1200, 1500, 1800
Corresponding fluid inlet temperature T_{in} (K)	300, 300, 600, 900, 1200, 1500

gradually to 0 again at $\tau = 1$ and the shape of the curve is affected significantly by particle thermal radiation. The trends exhibited by θ and ϑ for all simulations are similar. It is important to control the highest temperature in packed pebble beds in engineering applications. Thus, the range of non-dimensional temperature ϑ can be used to quantify the degree of uniformity of particle temperature

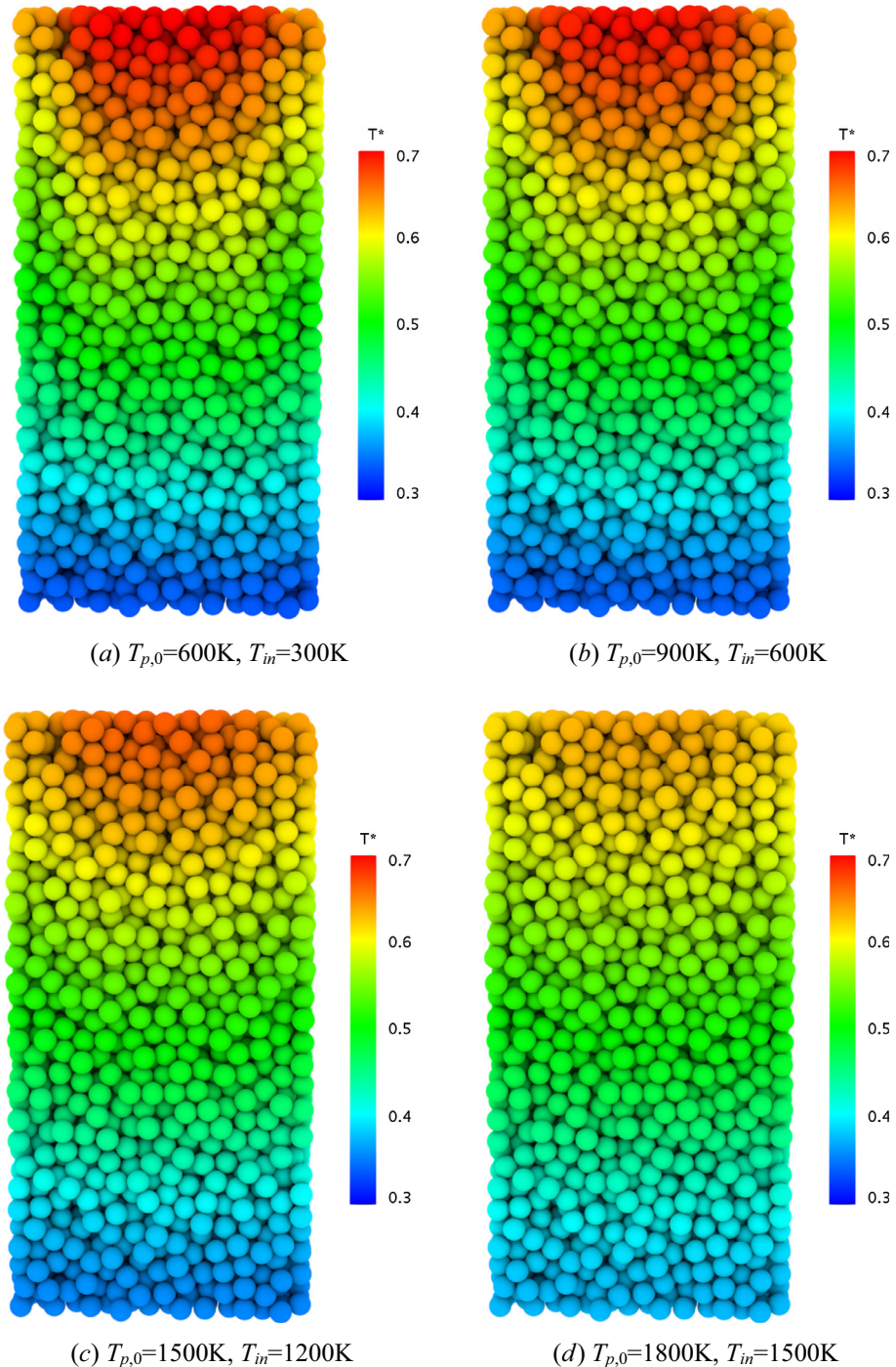


Fig. 5. Non-dimensional temperature field at non-dimensional temperature drop $\tau = 0.5$ and Nusselt number $Nu = 30$ with different initial temperatures of the packed pebble bed (sectional view at half width; here $Nu = \text{constant}$ is to keep the same convection and compare radiation).

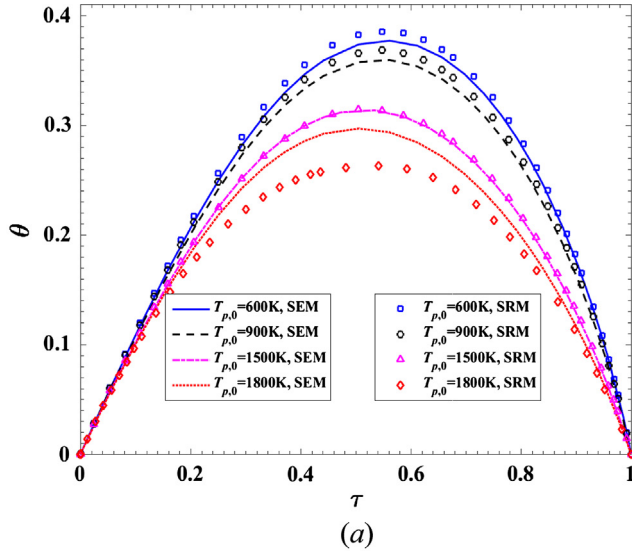
field. The range θ is also affected by heat convection and its maximum θ_{\max} increases significantly at high Nusselt numbers as seen in Fig. 7. θ_{\max} drops from 0.39 (0.382[▲]) at 400 K to 0.31 (0.314) at 1500 K and 0.26 (0.29) at 1800 K for $Nu = 30$. For $Nu = 60$ it reduces to 0.53 (0.544) at 1800 K from 0.66 (0.648) at 400 K. However, by visual inspection, the difference between the curves for different Nusselt numbers almost remains constant. It can be explained that heat convection is hardly influenced by temperature. Let the particle radiation factor φ be defined as

$$\varphi = \theta_{\max,c} - \theta_{\max} \quad (41)$$

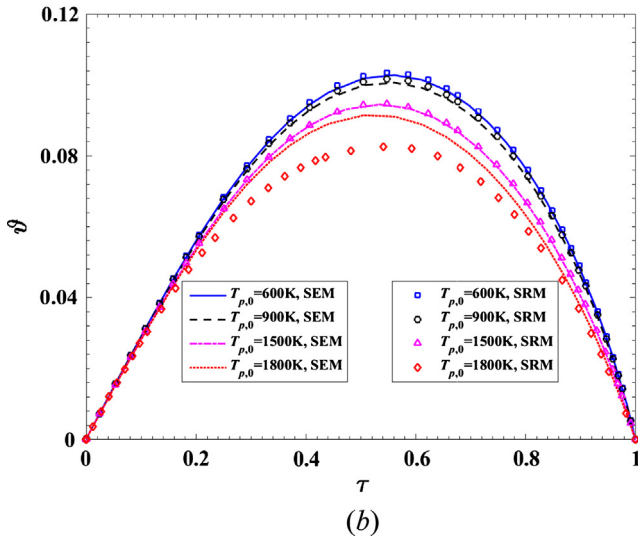
where $\theta_{\max,c}$ is the maximum of the range without any particle thermal radiation. From the numerical results shown in Fig. 8, the Nusselt number contributes little to the particle radiation factor and φ increases from almost 0 at 400 K to 0.055 (0.055) at 1200 K and about 0.13 (0.1) at 1800 K. Thus the particle radiation factor φ is an independent parameter that can be used to qualify the effect of particle radiation in a packed pebble bed.

3.4. Effect of fluid physical properties

It must be noted that the effect of the fluid physical properties on particle radiation in packed beds should also be considered. The



(a)



(b)

Fig. 6. Numerical results of the range (a) and standard deviation (b) of non-dimensional particle temperature for the packed pebble bed with different initial temperatures at $Nu = 30$.

Table 3
The function $\tau = f(\theta_{\max})$ of Fig. 6.

$T_{p,0} = 600\text{ K}$	$\theta_{\max} = 0.377$, $\tau = f(\theta_{\max}) = 0.56$	$\tau = 0.5$, $\theta = 0.373$
$T_{p,0} = 900\text{ K}$	$\theta_{\max} = 0.360$, $\tau = f(\theta_{\max}) = 0.53$	$\tau = 0.5$, $\theta = 0.357$
$T_{p,0} = 1500\text{ K}$	$\theta_{\max} = 0.314$, $\tau = f(\theta_{\max}) = 0.505$	$\tau = 0.5$, $\theta = 0.313$
$T_{p,0} = 1800\text{ K}$	$\theta_{\max} = 0.29$, $\tau = f(\theta_{\max}) = 0.505$	$\tau = 0.5$, $\theta = 0.29$

fluid density will increase significantly at high pressures, which contributes to a higher heat storage capacity of the fluid. The thermal conductivity, which is the ability of the gas to conduct heat, also varies greatly for different gases, from $0.015\text{ W}/(\text{m K})$ for carbon dioxide and $0.0242\text{ W}/(\text{m K})$ for air to $0.142\text{ W}/(\text{m K})$ for helium. Thus, the fluid density and thermal conductivity have been chosen as the basic parameters. Only air at standard conditions was used in the previous cases, although the coolant in a HTGR is helium at 3.0 MPa . In Fig. 9a it can be seen that as the fluid density increases from 1.225 kg/m^3 to 2.0 kg/m^3 , 4.0 kg/m^3 and 5.0 kg/m^3 , the particle radiation factor φ tends to decrease gradually. The same tendency is also observed in Fig. 9b in the cases where the thermal conductivity increases from $0.0242\text{ W}/(\text{m K})$ to $1\text{ W}/(\text{m K})$, $0.08\text{ W}/$

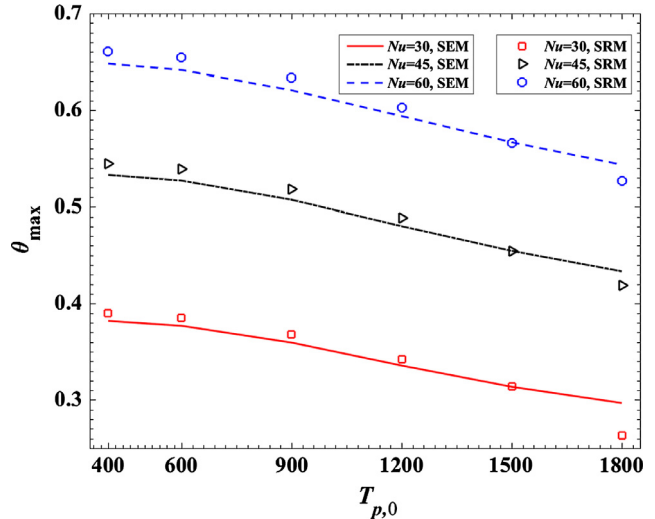


Fig. 7. The range of non-dimensional particle temperature for the packed pebble bed at different Nusselt numbers.

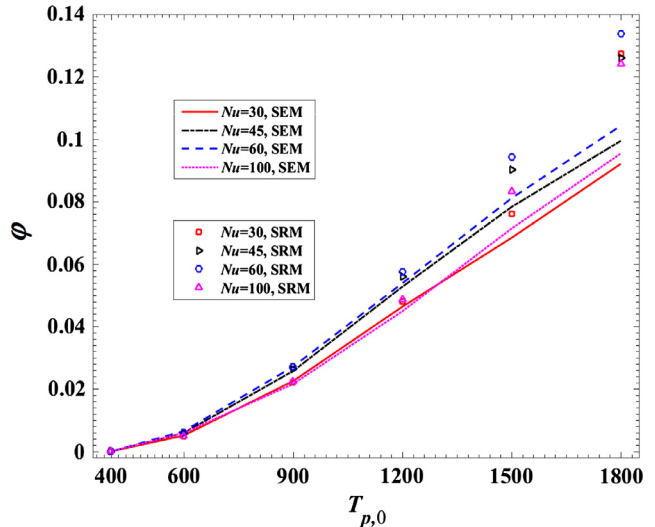


Fig. 8. Particle radiation factor for packed pebble bed at different Nusselt numbers.

(m K) and $0.1\text{ W}/(\text{m K})$. It means that when the fluid heat storage capacity or the thermal conductivity is larger, the non-uniformity of the temperature in the packed pebble bed is less.

In addition, from Figs. 6–9, it is confirmed that the above conclusions can be derived either from the SRM or the SEM model. For example, in Fig. 8, although the results obtained from the SRM model are somewhat higher than the results of the SEM model, they both lead to the same conclusion that the particle radiation factor φ is almost independent of the Nusselt number. In addition, as the SRM model is not so good for radiation prediction at high temperature, it is quite necessary to improve it in high temperature ranges. Therefore, in the following applications, the SRM+ model (an improved version of the SRM model at high temperature) is used for the HTR-10 reactor.

4. Applications

4.1. Steady state analysis

The HTR-10, which is an experimental nuclear reactor with the thermal power of 10 MW [6], was built by the institute of nuclear

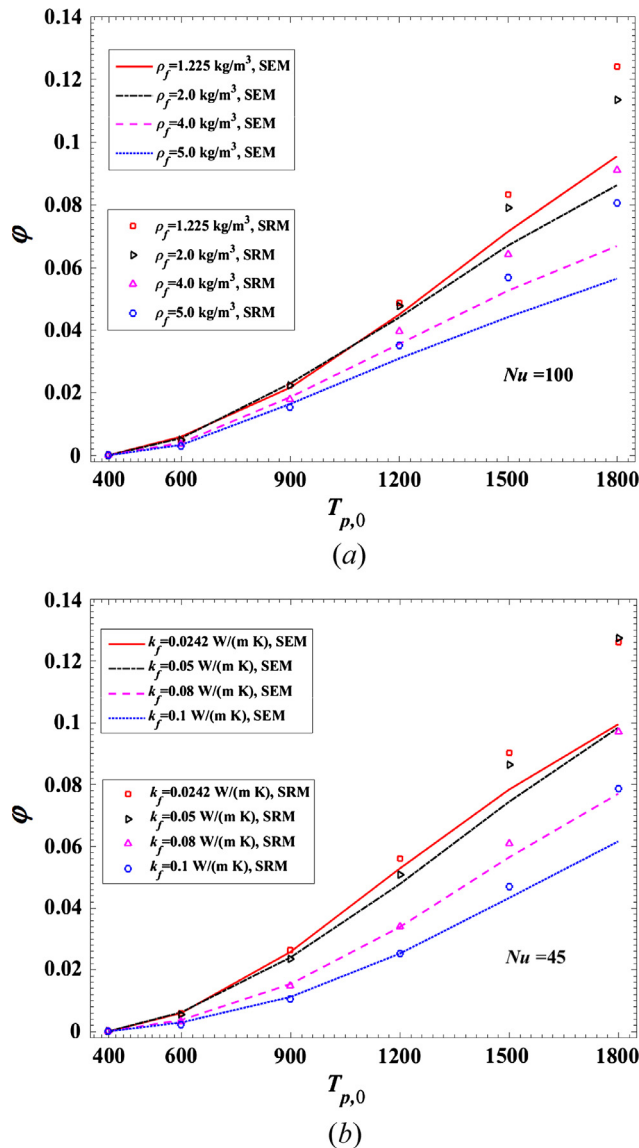


Fig. 9. Effect of fluid density (a) and thermal conductivity (b) on particle radiation factor for the packed pebble bed.

and new energy technology (INET) in 2001. The HTGR demonstration project known as the HTR-PM is now under construction. However, until now, experimental tests related to neutron dynamics [18] and thermal hydraulics [4] have been only performed in the HTR-10. Thus the core of HTR-10, which has an equivalent diameter of 1.8 m and an average height of 1.97 m and is filled with 27,000 spheres, was selected for our simulations. The short-range radiation model was also applied for comparison in simulations. It is noted that the Eq. (22) in the short-range radiation model for particle radiation needs to be modified when the temperature exceeds 1400 K, and the heat flux can be re-written as

$$q_{r,ik} = q_{no} [0.67 + 0.33 \exp(-2.855(T_a/T_z - 1))] \quad (42)$$

where q_{no} is the value calculated by Eq. (22), $T_a = (T_i + T_j)/2$ and $T_z = 1400$ K. Herein the previous "SRM" model with Eq. (22) replaced by Eq. (42) is renamed as a "SRM+" model, and used hereafter for the HTR-10. The KTA standards based experimental results (Table 1) is used as the correlation for the fluid-particle convection. The pressure drop according to the KTA standards [6] is formulated as

$$\frac{\Delta P}{\Delta L} = \left(\frac{320}{Re_h} + \frac{6}{Re_h^{0.1}} \right) \frac{1 - \alpha_f}{\alpha_f^3} \frac{1}{2\rho d_p} \left(\frac{Q_m}{A} \right)^2 \quad (43)$$

where $Q_m = \rho_f u_f \alpha_f A$ is fluid mass flow rate and A is the sectional area of packed pebble bed perpendicular to the flow direction, Re_h is effective Reynolds number and $Re_h = Q_m d_p / [A \mu_f (1 - \alpha_f)]$. This correlation is applied in the momentum source term by $S_m = \alpha_f \Delta P / \Delta L$.

The HTR-10 benchmark problem is based on an initial core under full power [21], in which no fission energy is released for $z > 1.7$ m, where z is the distance to the top. The coolant (helium gas) at 250 °C under 3.0 MPa flows into the core at the top whose mass flow rate is 3.77 kg/s [6]. Thus, a uniform velocity with constant temperature was set at the top, and the outflow boundary condition was set at the bottom. The non-slip and adiabatic wall boundary condition was used on the walls. It was assumed that heat source of all particles in the region that the energy was released was uniform. A simple mesh was employed and the temperature distribution that was obtained at steady state is shown in Fig. 10. The temperature increases along the flow direction and reaches its maximum of about 850 °C at $z = 1.7$ m. By comparison with the results predicted by other empirical codes [21] shown in Fig. 11a, it can be seen that results predicted by the present model are in general agreement with the results obtained by VSOP and TINTE. However, the results obtained by THERMIX are slightly higher with the highest temperature being about 920 °C. This could be caused by the conservative formulation employed by THERMIX used for nuclear safety analysis. It is also shown in Fig. 11b that the results obtained from the short-range radiation model are in good agreement with those from the semi-empirical radiation model.

When full power for the initial core is achieved, a transition to the equilibrium core is carried out dynamically and all particles in the packed pebble become fuel elements [6]. With an increase in coolant flow rate, the pressure drop over the packed pebble bed increases significantly as shown in Fig. 12a. Also, the pressure drop through other components in the reactor such as reflector, hot gas duct and steam generator will also increase. From the perspective of heat transfer, it is shown in Fig. 12b that increasing the mass flow rate can increase the heat convection capability and decrease the coolant outlet temperature. This trend is especially clear at the low mass flow rates. It is also shown that when the reactor is operated in low power levels (such as 50% and 80% full power), the coolant outlet temperature is not very high even at very low mass flow rates. The temperature is about 770 °C when the coolant flow rate decreases to 1.9 kg/s at 50% full power. In this case, it is possible to decrease the coolant flow rate of the reactor to a low level and save the fans power significantly, which is also benefit for the control systems. On the contrary, at high power levels (e.g. 120% and 150% full power), a much higher flow rate is needed to control the coolant outlet temperature under a reasonable limit. In that case, the pressure drops and the fans power for driving the coolant will increase significantly, which may also bring trouble to the control systems, or even make the nuclear reactor unsafe.

4.2. Decay heat removal

Unlike traditional coal-fired power plants and hydropower stations, decay heat removal after shut-down is an important issue to consider in the design of high temperature gas-cooled reactors. In a conservative model for nuclear safety, it is assumed that there is no coolant convection heat transport and only particle-particle conduction and thermal radiation are available for heat removal. The effective thermal conductivity for conduction (k_c) and radiation (k_r) become key parameters to represent the ability for decay heat removal in a HTGR [22,25]. Although the solid conductivity of par-

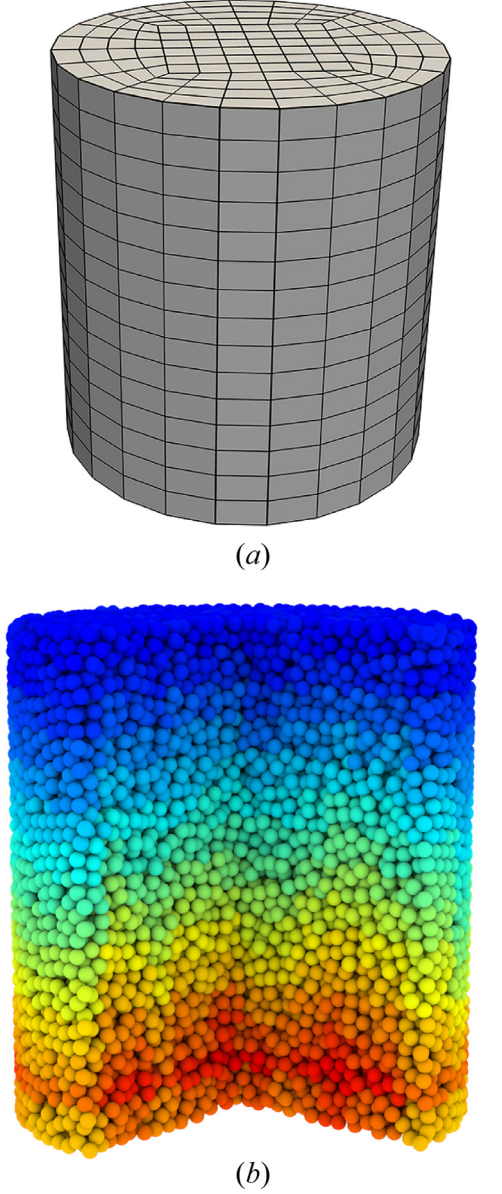


Fig. 10. CFD mesh for the core of HTR-10 (a) and particle surface temperature field (b) at full power of initial core (sectional view).

ticle and thermal conductivity of gas are functions of temperature, the effective thermal conductivity for particle conduction is almost the same at high temperature [26]. Thus, it is approximated that the heat conduction between particles is not affected by temperature. The conduction part (k_c) can be obtained from experimental data under normal or elevated temperatures.

In the current radiation model, a packed pebble bed of the HTR-10 without coolant convection at a very low thermal power was investigated to compute the radiation contribution (k_r). Here, radiation is considered in the way of effective thermal conduction. Hence, the top and bottom walls were assumed to be adiabatic and the temperature at the outer wall was assumed to be constant. In a pseudo-porous media model, the radial temperature distribution with constant conductivity and uniform heat source can be written as

$$T(x) = T_w + \frac{P_s}{4V_b k_{eff}} (R_o^2 - x^2) \quad (44)$$

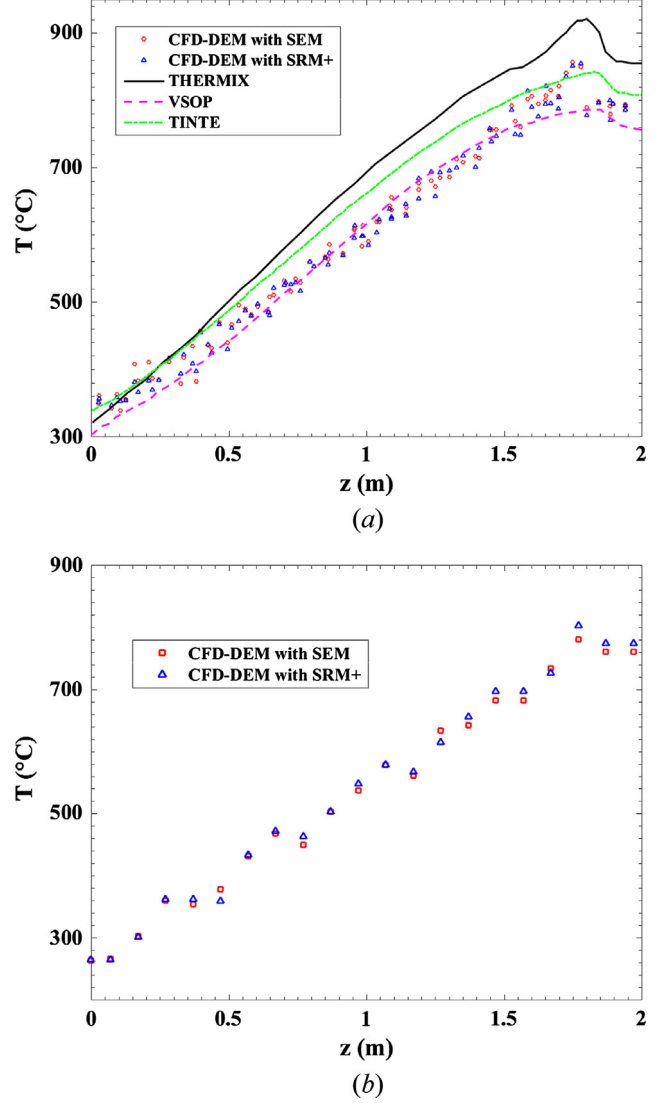


Fig. 11. The particle surface temperature with semi-empirical radiation model (a) and fluid temperature (b) on the centerline alone the flow direction at full power of initial core for the HTR-10.

where T_w is the wall temperature at the outer wall and x is the distance to the center line. R_o , P_s and V_b are the outer diameter, total heat source power and volume of the packed pebble bed. k_{eff} is the effective thermal conductivity which includes conduction and radiation and $k_r = k_{eff} - k_c$. There is a linear relationship between $T(x)$ and x^2 , which is proportional to the effective thermal conductivity. This trend is also observed in the simulation results shown in Fig. 13. The values of k_r (see Fig. 14) can be obtained using the least squares method for post-processing of the simulation data. When it is within the super-high temperature region ($T > 1262^\circ\text{C}$ ($A > 1$)), k_r obtained from the SRM model without modification is slightly higher than the others. However, even for $T > 1262^\circ\text{C}$, it can be seen in Fig. 14 that k_r under different wall temperatures predicted by the SRM+ model is in good agreement with the predicted values obtained using the empirical correlations, which are described in Wu et al. [30]. Particle radiation increases markedly with an increase in the temperature. It can be seen in Fig. 14 that k_r increases from $0.4 \text{ W}/(\text{m}^\circ\text{C})$ at 100°C to $10.5 \text{ W}/(\text{m}^\circ\text{C})$ at 800°C and $44.6 \text{ W}/(\text{m}^\circ\text{C})$ at 1600°C , which enhances the ability of the pebble bed to remove the decay heat at high temperatures significantly.

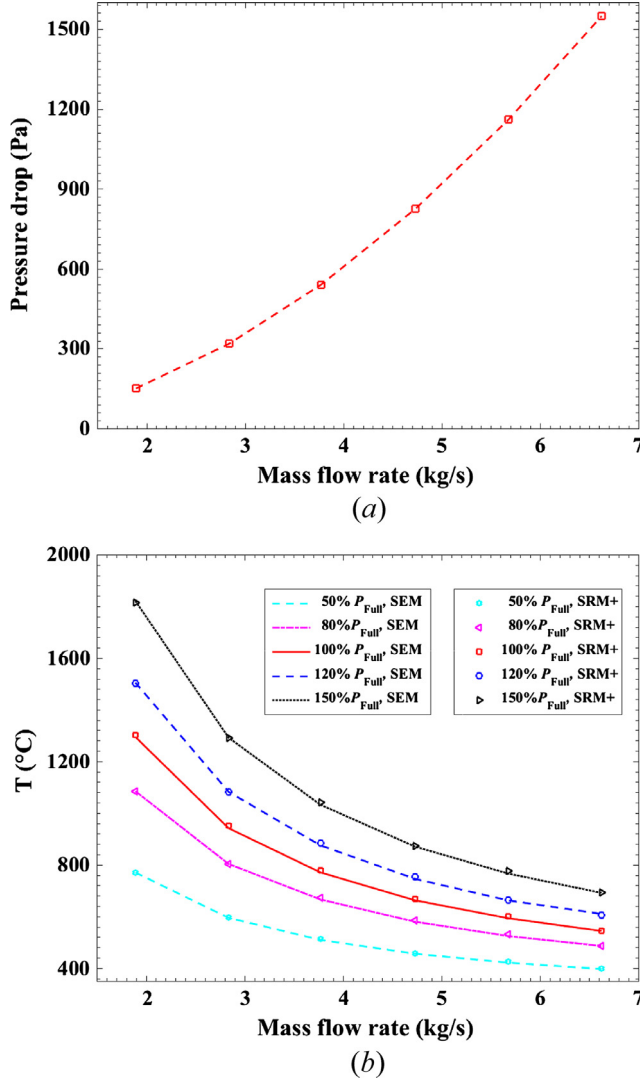


Fig. 12. The pressure drop in the packed pebble bed (a) and coolant outlet temperature of the equilibrium core at different power levels (b).

The decay heat power (P_d) with time is showed in Fig. 15a [7]. It can be seen that the decay heat decreases from about 5.6% full power at shut-down to 1% at 2 h and 0.5% at 30 h. It is assumed that decay heat is uniformly distributed in the packed pebble bed. However, the heat generated at localized spots may be higher than the average, therefore the reactor with 150% P_d and 200% P_d were also considered. At the start of the transient simulation, all particles and the wall were assumed conservatively at 920 °C, which is the highest temperature at steady state predicted by THERMIX code. Fig. 15b shows the highest temperature in the packed bed as a function of time for the case when radiation is neglected, as well as when radiation is accounted for. It can be seen that the temperature will reach a maximum value of 1405 °C at 100% P_d , 1646 °C at 150% P_d and 1888 °C at 200% P_d at about 38 h when particle radiation is not considered. However, when particle radiation is taken into account, the maximum temperature decreases to 1069 °C (1059 °C) at 100% P_d , 1133 °C (1122 °C) at 100% P_d and 1192 °C (1181 °C) at 100% P_d , which are still safe for the nuclear reactor.

It can be concluded that, in spite of using the short-range model (SRM or SRM+) or the empirical model for radiation, the present CFD-DEM model coupled with particle radiation is suitable for the prediction and analysis of heat transfer in real reactors, which

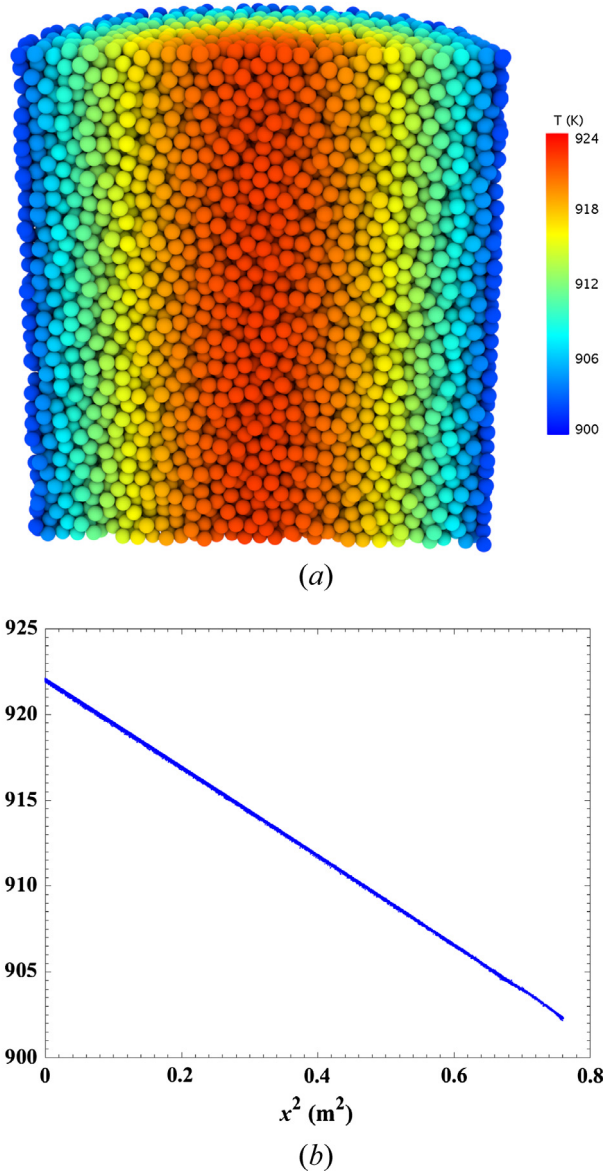


Fig. 13. The sectional view (a) and radial distribution (b) of temperature in the packed pebble bed at steady state without coolant convection (wall temperature $T_w = 900$ K, $k_c = 4.0$ W/m°C and heat source power $P_s = 5.4$ kW with uniform distribution).

is essential and significant for reactor design and improvement. Similarly, the present model can also be potentially used for other engineering applications with radiation at high temperatures.

5. Conclusions

A complete CFD-DEM method considering particle motion, fluid flow, particle-fluid interactions and heat convection, conduction and particle radiation was developed for packed pebble beds. In the particle radiation model, a short-range radiation model (SRM) or a modified short-range model (SRM+) is applied, which has been validated for practical applications. In order to explore the effect of particle thermal radiation on the flow and heat transport processes in packed pebble beds, simulations of different cases with different initial conditions or physical properties were performed. Moreover, the performance of the HTR-10 under steady

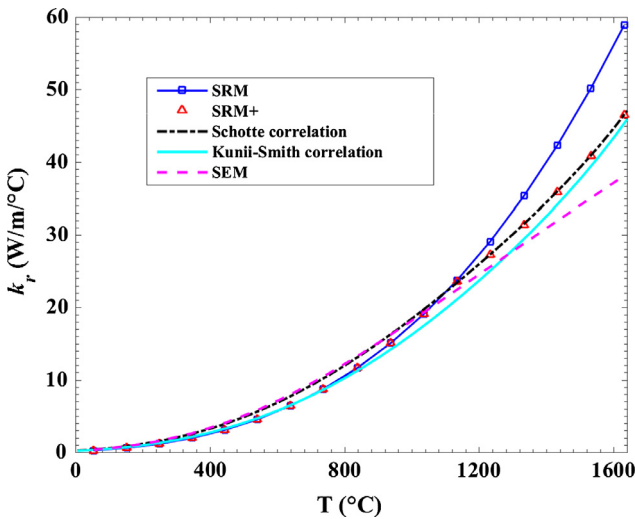
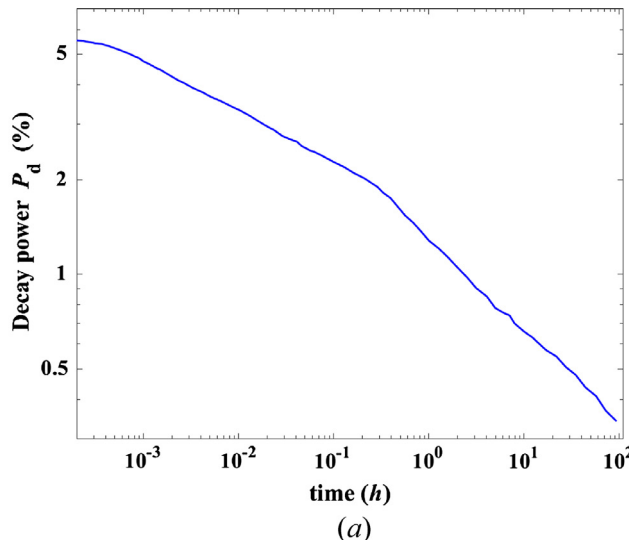
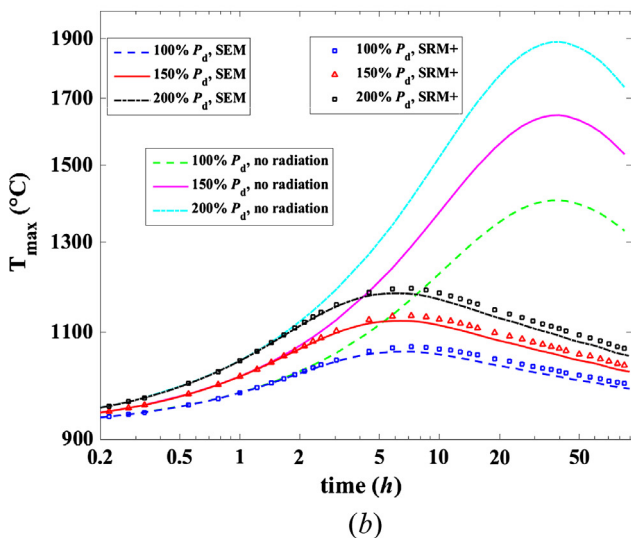


Fig. 14. The effective thermal conductivity for radiation (k_r) of the equivalent HTR-10 core as a function of temperature (T is the average temperature of the packed pebble bed).



(a)



(b)

Fig. 15. The decay heat power after shut down of HTR-10 (a) and the time evolution of the highest temperature (b).

state full power and the performance under decay heat removal were investigated. It has been found that:

- (1) For the three basic modes of heat transfer, namely conduction between particles at contact, fluid-particle convection and particle thermal radiation, particle thermal radiation increases significantly at high temperatures. Radiation enhances the heat transfer significantly and the particle temperature field in a packed pebble bed tends to be much more uniform.
- (2) Using dimensional analysis, a particle radiation factor φ can be defined. It is an independent parameter that can be used to qualify the effect of particle radiation in a packed pebble bed. The particle radiation factor increases significantly with the temperature from almost 0 at 400 K to 0.055 at 1200 K and about 0.13 (0.1) at 1800 K, and is hardly affected by conduction and convection heat transfer.
- (3) Some fluid physical properties also make contribution to the effect of particle radiation. For example, the fluid density increases with an increase in pressure and the thermal conductivity varies for different gases. It was shown that the particle radiation factor decreases gradually when the heat storage capacity or thermal conductivity of the fluid increase. Additionally, although other fluid properties which are functions of varied temperatures may also influence particle radiation in HTGRs through the Reynolds number or Prandtl number, they are not as important as the fluid density and thermal conductivity.
- (4) The numerical results obtained with the SRM+ model for the HTR-10 benchmark problem are in general in good agreement with the results obtained by the empirical codes. It was shown that when the reactor is operated above full power, the power required by the fans to drive the convective flow will increase significantly and it may be a challenge to ensure the nuclear safety of the control systems. In the removal of the decay heat of HTR-10, particle radiation plays an important role to maintain temperature below the maximum allowable level. This application demonstrates the potential utilization of present model for the prediction of particle radiation and the analysis of many practical heat transfer devices.

Acknowledgments

The authors are grateful for the support of this research by the National Natural Science Foundations of China (Grant No. 51576211), the Science Fund for Creative Research Groups of National Natural Science Foundation of China (Grant No. 51321002), the National High Technology Research and Development Program of China (863) (2014AA052701), and the Foundation for the Author of National Excellent Doctoral Dissertation of PR China (Grant No. 201438). This work is also supported financially by China Scholarship Council (CSC) under the Grant No. 201506210365.

References

- [1] R.S. Abdulmohsin, M.H. Al-Dahhan, Characteristics of convective heat transport in a packed pebble-bed reactor, Nucl. Eng. Des. 284 (2015) 143–152.
- [2] J. Ai, J.-F. Chen, J.M. Rotter, J.Y. Ooi, Assessment of rolling resistance models in discrete element simulations, Powder Technol. 206 (2011) 269–282.
- [3] M. Bahrami, M.M. Yovanovich, J.R. Culham, Effective thermal conductivity of rough spherical packed beds, Int. J. Heat Mass Transfer 49 (2006) 3691–3701.
- [4] F. Chen, Y. Dong, Y. Zheng, L. Shi, Z. Zhang, Benchmark calculation for the steady-state temperature distribution of the HTR-10 under full-power operation, J. Nucl. Sci. Technol. 46 (2009) 572–580.

- [5] P.A. Cundall, O.D.L. Strack, A discrete numerical model for granular assemblies, *Geotechnique* 29 (1979) 47–65.
- [6] Z. Gao, L. Shi, Thermal hydraulic calculation of the HTR-10 for the initial and equilibrium core, *Nucl. Eng. Des.* 218 (2002) 51–64.
- [7] Z. Gao, L. Shi, Thermal hydraulic transient analysis of the HTR-10, *Nucl. Eng. Des.* 218 (2002) 65–80.
- [8] N.T. Grier, Tabulations of Configuration Factors between Any Two Spheres and Their Parts, Washington, DC, 1969.
- [9] N. Gui, J. Fan, Numerical study of heat conduction of granular particles in rotating wavy drums, *Int. J. Heat Mass Transfer* 84 (2015) 740–751.
- [10] N. Gui, J.R. Fan, K. Luo, DEM-LES study of 3-D bubbling fluidized bed with immersed tubes, *Chem. Eng. Sci.* 63 (2008) 3654–3663.
- [11] N. Gui, J.R. Fan, S. Chen, Numerical study of particle-particle collision in swirling jets: a DEM-DNS coupling simulation, *Chem. Eng. Sci.* 65 (2010) 3268–3278.
- [12] J.E. Hilton, L.R. Mason, P.W. Cleary, Dynamics of gas-solid fluidised beds with non-spherical particle geometry, *Chem. Eng. Sci.* 65 (2010) 1584–1596.
- [13] Q.F. Hou, Z.Y. Zhou, A.B. Yu, Gas-solid flow and heat transfer in fluidized beds with tubes: Effects of material properties and tube array settings, *Powder Technol.* 296 (2016) 59–71.
- [14] S. Just, G. Toschkoff, A. Funke, D. Djuric, G. Scharrer, J. Khinast, K. Knop, P. Kleinebudde, Experimental analysis of tablet properties for discrete element modeling of an active coating process, *Off. J. Am. Assoc. Pharm. Scient.* 14 (2013) 402–411.
- [15] C. Kloss, C. Goniva, A. Hager, S. Amberger, S. Pirker, Models, algorithms and validation for opensource DEM and CFD-DEM, *Prog. Comput. Fluid Dynam.*, *Int. J.* 12 (2012) 140.
- [16] B. Krause, B. Liedmann, J. Wiese, S. Wirtz, V. Scherer, Coupled three dimensional DEM-CFD simulation of a lime shaft kiln—Calcination, particle movement and gas phase flow field, *Chem. Eng. Sci.* 134 (2015) 834–849.
- [17] KTA Standards, Reactor Core Design of High-Temperature Gas-Cooled Reactors Part 2: Heat Transfer in Spherical Fuel Elements, Nuclear Safety Standards Commission, Salzgitter, Germany (3102.3), 1983.
- [18] K. Kunitomi, Y. Sun, S. Ball, H. Brey, M. Methnani, Evaluation of High Temperature Gas Cooled Reactor Performance: Benchmark Analysis Related to Initial Testing of the HTTR and HTR-10 IAEA-TEDOC-1382, International Atomic Energy Agency, 2003.
- [19] J. Li, D. Mason, A computational investigation of transient heat transfer in pneumatic transport of granular particles, *Powder Technol.* 112 (2000) 273–282.
- [20] Y. Li, W. Ji, Acceleration of coupled granular flow and fluid flow simulations in pebble bed energy systems, *Nucl. Eng. Des.* 258 (2013) 275–283.
- [21] M. Methnani, B. Tyobeka, Evaluation of High Temperature Gas Cooled Reactor Performance: Benchmark analysis related to the PBMR-400, PBMM, GT-MHR, HTR-10 and the ASTRA Critical Facility IAEA-TECDOC-1694, International Atomic Energy Agency, 2006.
- [22] H. Niessen, S. Ball, Heat Transport and Afterheat Removal for Gas Cooled Reactors under Accident Conditions IAEA-TECDOC-1163, International Atomic Energy Agency, 2000.
- [23] B. Singh, M. Kaviany, Effect of solid conductivity on radiative heat transfer in packed beds, *Int. J. Heat Mass Transfer* 37 (1994) 2579–2583.
- [24] T. Tsory, N. Ben-Jacob, T. Brosh, A. Levy, Thermal DEM–CFD modeling and simulation of heat transfer through packed bed, *Powder Technol.* 244 (2013) 52–60.
- [25] W. van Antwerpen, C.G. du Toit, P.G. Rousseau, A review of correlations to model the packing structure and effective thermal conductivity in packed beds of mono-sized spherical particles, *Nucl. Eng. Des.* 240 (2010) 1803–1818.
- [26] W. van Antwerpen, P.G. Rousseau, C.G. du Toit, Multi-sphere unit cell model to calculate the effective thermal conductivity in packed pebble beds of mono-sized spheres, *Nucl. Eng. Des.* 247 (2012) 183–201.
- [27] W.L. Vargas, J. McCarthy, Conductivity of granular media with stagnant interstitial fluids via thermal particle dynamics simulation, *Int. J. Heat Mass Transfer* 45 (2002) 4847–4856.
- [28] H. Wahyudi, K. Chu, A. Yu, 3D particle-scale modeling of gas–solids flow and heat transfer in fluidized beds with an immersed tube, *Int. J. Heat Mass Transfer* 97 (2016) 521–537.
- [29] D. Wen, Y. Ding, Heat transfer of gas flow through a packed bed, *Chem. Eng. Sci.* 61 (2006) 3532–3542.
- [30] H. Wu, N. Gui, X. Yang, J. Tu, S. Jiang, Effect of scale on the modeling of radiation heat transfer in packed pebble beds, *Int. J. Heat Mass Transfer* 101 (2016) 562–569.
- [31] Z. Wu, D. Lin, D. Zhong, The design features of the HTR-10, *Nucl. Eng. Des.* 218 (2002) 25–32.
- [32] S. Yagi, D. Kunii, Studies on effective thermal conductivities in packed beds, *AIChE J.* 3 (1957) 373–381.
- [33] W.J. Yang, Z.Y. Zhou, A.B. Yu, Particle scale studies of heat transfer in a moving bed, *Powder Technol.* 281 (2015) 99–111.
- [34] Z. Zhang, Z. Wu, D. Wang, Y. Xu, Y. Sun, F. Li, Y. Dong, Current status and technical description of Chinese 2 × 250 MWth HTR-PM demonstration plant, *Nucl. Eng. Des.* 239 (2009) 1212–1219.
- [35] Y. Zhao, M. Jiang, Y. Liu, J. Zheng, Particle-scale simulation of the flow and heat transfer behaviors in fluidized bed with immersed tube, *AIChE J.* 55 (2009) 3109–3124.
- [36] Y. Zheng, J. Lapins, E. Laurien, L. Shi, Z. Zhang, Thermal hydraulic analysis of a pebble-bed modular high temperature gas-cooled reactor with ATTICA3D and THERMIX codes, *Nucl. Eng. Des.* 246 (2012) 286–297.
- [37] W. Zhong, A.B. Yu, G. Zhou, J. Xie, H. Zhang, CFD simulation of dense particulate reaction system: approaches, recent advances and applications, *Chem. Eng. Sci.* 140 (2016) 16–43.
- [38] Z.Y. Zhou, S.B. Kuang, K.W. Chu, A.B. Yu, Discrete particle simulation of particle–fluid flow: model formulations and their applicability, *J. Fluid Mech.* 661 (2010) 482–510.
- [39] Z.Y. Zhou, D. Pinson, R.P. Zou, A.B. Yu, Discrete particle simulation of gas fluidization of ellipsoidal particles, *Chem. Eng. Sci.* 66 (2011) 6128–6145.
- [40] Z.Y. Zhou, A.B. Yu, P. Zulli, Particle scale study of heat transfer in packed and bubbling fluidized beds, *AIChE J.* 55 (2009) 868–884.
- [41] Z.Y. Zhou, A.B. Yu, P. Zulli, A new computational method for studying heat transfer in fluid bed reactors, *Powder Technol.* 197 (2010) 102–110.
- [42] H.P. Zhu, Z.Y. Zhou, R.Y. Yang, A.B. Yu, Discrete particle simulation of particulate systems: theoretical developments, *Chem. Eng. Sci.* 62 (2007) 3378–3396.